FRASA: Feedback Retransmission Approximation for the Stability Region of Finite-User Slotted ALOHA

Ka-Hung Hui, *Student Member, IEEE*, On-Ching Yue, *Senior Member, IEEE*, and Wing-Cheong Lau, *Senior Member, IEEE*

***Abstract*—FRASA, *Feedback Retransmission Approximation for Slotted ALOHA*, is proposed to study the stability region of finite-user slotted ALOHA under the collision channel. With FRASA, the stability region is derived in *closed form* for *any* number of users in the system. The result derived from FRASA is shown to be identical to the analytical result of finite-user slotted ALOHA when there are two users. It is shown that the stability region obtained from FRASA is a good *approximation* to the stability region of finite-user slotted ALOHA. The *convex hull bound*, which is convex, piecewise linear and outer-bounds the stability region of FRASA, is provided. *p-convexity*, an essential property that the stability region of FRASA should have to ensure the convex hull bound to be close to the boundary, is characterized. From these, it is derived that the stability region of FRASA can never be convex when there are more than two users. A separate convex and piecewise linear inner bound on the stability region of FRASA, *the supporting hyperplane bound*, is also given. More insights on the characterization of the capacity region of other types of wireless random access networks can be obtained from the analytical findings with FRASA.**

***Index Terms*—Stability Region, Random Access, Slotted ALOHA, FRASA.**

I. Introduction

THE study of the stability region of slotted ALOHA has attracted many researchers [1]–[12]. Despite the simplicity of slotted ALOHA, this problem is extremely difficult when M, the number of users in the system, exceeds two, even on the collision channel assumption. Under this assumption, successful transmissions occur if and only if there is one active transmitter, because of the interference among the stations. The inherent difficulty in the analysis is due to the effect of queueing in each transmitter. More specifically, the probability of successful transmission depends on the number of active transmitters, which in turn depends on whether the queues in the transmitters are empty or not. However, it is still an open problem to obtain the stationary joint queue statistics in closed form.

Instead of finding the exact stability region, previous researchers have attempted to bound the stability region [1]–[3], [6], [8]. However, they did not require the bounds to be *convex* or *piecewise linear*, which are important in traffic engineering [13]. Requiring such properties reduces the traffic engineering problem into convex or linear programming, which are relatively more tractable. Therefore, we are motivated to derive convex and piecewise linear bounds on the stability region. We hope this work can serve as a basis and can be extended to consider multi-hop networks and interference models other than the collision channel.

In this paper, we propose FRASA, *Feedback Retransmission Approximation for Slotted ALOHA*, as a surrogate to approximate finite-user slotted ALOHA. By considering FRASA, we make the following contributions:

1) We obtain in *closed form* the boundary of the stability region of FRASA under the collision channel for *any* number of users in Section III. The result obtained from FRASA is identical to the analytical result of finite-user slotted ALOHA for $M = 2$.
2) We demonstrate by simulation in Section IV that the stability region obtained from FRASA is a good approximation to the stability region of finite-user slotted ALOHA. We also demonstrate that FRASA has a wider range of applicability than the existing bounds.
3) In Section V we provide a *convex hull bound*, which is convex, piecewise linear and outer-bounds the stability region of FRASA. This bound can be computed by using the transmission probability vector only. In Section VI we introduce ***p*-convexity**, which is essential to ensure the convex hull bound to be close to the boundary of the stability region of FRASA. The nonconvexity of the stability region of FRASA when $M > 2$ follows from these results.
4) A convex and piecewise linear inner bound on the stability region of FRASA, called the *supporting hyperplane bound*, is given in Section VII.

For the rest of the paper, we present related works in Section II. In Section VIII we conclude the paper and discuss future works.

II. Related Works

The study of the stability region of M-user infinite-buffer slotted ALOHA was initiated by [1] decades before, and is still an ongoing research. The authors in [1] obtained the exact stability region when $M = 2$ under the collision channel. [2]

Manuscript received XXX YY, ZZZZ; revised XXX YY, ZZZZ. The material in this paper was presented in part at the 15th IEEE International Conference on Network Protocols, Beijing, China, October, 2007.

K.-H. Hui is with the Department of Electrical Engineering and Computer Science at Northwestern University, Evanston, IL 60208, USA (e-mail: khhui@u.northwestern.edu).

O.-C. Yue and W.-C. Lau are with the Department of Information Engineering at The Chinese University of Hong Kong, Shatin, Hong Kong (e-mail: onching@ie.cuhk.edu.hk; wclau@ie.cuhk.edu.hk).

and [3] used *stochastic dominance* and derived the same result as in [1] for the case of $M = 2$.

For general M, there were attempts to find the exact stability region, but there was only limited success. [5] established the boundary of the stability region, but it involves stationary joint queue statistics, which still do not have closed form to date. [12] obtained in closed form a partial characterization on the boundary of the stability region under *partial interference*. [14] obtained the necessary and sufficient per-queue stability condition, which, unfortunately, can be computed analytically only for several special cases.

Instead, many researchers focused on finding bounds on the stability region for general M. [1] obtained separate sufficient and necessary conditions for stability. [2] and [3] derived tighter bounds on the stability region by using stochastic dominance in different ways. [6] introduced *instability rank* and used it to improve the bounds on the stability region. However, the bounds in [2] and [6] are not always applicable. Also, the bounds obtained may not be piecewise linear.

With the advances in multi-user detection, researchers also studied this problem with the *multipacket reception* (MPR) model. [7] studied this problem in the infinite-user, single-buffer and symmetric MPR case. [8] considered the problem with finite users and infinite buffer. They obtained the boundary for the asymmetric MPR case with two users, and also the inner bound on the stability region for general M. [9] obtained an outer bound on the stability region by using the positive and strong positive correlation properties of the stationary distribution of the queue lengths.

Recently there were a few works on approximating the stability region of slotted ALOHA. [10] used *mean field analysis* to approximate the stability region of slotted ALOHA and showed that it is asymptotically exact as the number of users grow to infinity. [11] used *ellipsoids* to approximate the stability region of slotted ALOHA.

III. The FRASA Model

In slotted ALOHA, there is a queue of infinite buffer at each transmitter. Packet arrivals are assumed to be Bernoulli. When a packet arrives, it joins the end of the queue. The head-of-line packet is transmitted when the transmitter decides to transmit, and it remains at head-of-line until it is successfully transmitted. This is depicted in the upper part of Fig. 1.

Due to the complexity introduced by the queues, we propose FRASA, *Feedback Retransmission Approximation for Slotted ALOHA*, as a surrogate to approximate finite-user slotted ALOHA. In FRASA, the buffer in each transmitter can hold one packet only. Whenever there is a packet in the buffer, if the transmitter decides not to transmit the packet, or the transmitter cannot successfully transmit the packet due to collision, the packet will be removed from the buffer and put back in the buffer again in the earliest slot that has no new arrivals. Since the arrivals are Bernoulli, a retransmitted packet can be considered to suffer a geometrically distributed random delay before it is put back in the buffer. Because of the temporal correlation between the new arrivals and the retransmissions, the aggregate arrival (which includes the new arrivals and the retransmissions) is not memoryless. Nevertheless, the aggregate arrival is *assumed* to be Bernoulli or memoryless for analytical tractability. Similar approximation was introduced by [15]. FRASA is shown in the lower part of Fig. 1.

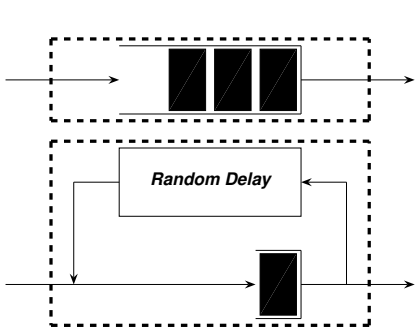

Fig. 1. Slotted ALOHA model: (Upper) Original; (Lower) FRASA.

Notice that the slotted ALOHA and FRASA systems are similar in many ways. First, both define stability as the situation that the number of packets in the transmitter of each link does not grow to infinity. Second, if both systems have the same initial condition, the arrival processes in both systems are the same, and in every time slot, the transmission attempts of all links are the same for both systems, then the number of packets in the transmitter of each link are the same for both systems, except for a subtle difference: in slotted ALOHA the packets are located in the queue, while in FRASA, the packets are in the feedback loop. Also, the probability that there is a packet in the buffer are similar for both systems: when both systems are stable, the queue in slotted ALOHA and the single buffer in FRASA can be empty; on the other hand, when both systems are unstable, there is always a packet in the queue in slotted ALOHA, while the single buffer in FRASA is always occupied. In particular, we will show in the following section that, when the number of contenting users is equal to two, the stability regions of slotted ALOHA and FRASA are identical. Motivated by this finding, we speculate that the stability region of FRASA should be a good approximation to the stability region of slotted ALOHA in more general settings and we will validate this speculation via analysis and simulation in the remainder of this paper.

Assume there are M links in the network, and the set of links is denoted by $\mathcal{M} = \{n\}_{n=1}^{M}$. Let $\boldsymbol{\lambda} = (\lambda_n)_{n\in\mathcal{M}}$ and $\boldsymbol{p} = (p_n)_{n\in\mathcal{M}}$ be the arrival rate vector and the transmission probability vector respectively. Define $\overline{p}_n = 1 - p_n$ for all $n \in \mathcal{M}$. Let χ_n be the aggregate arrival rate of link $n \in \mathcal{M}$ where χ_n is between zero and one. For each $n \in \mathcal{M}$, the feedback loop can be considered as a server which is blocked (by new arrivals) with probability λ_n in each slot. A packet in the feedback loop is put back in the buffer once there is no new arrivals, which happens with probability $1 - \lambda_n$ in each slot. Therefore, we define the service rate of the feedback loop to be $1 - \lambda_n$. Denote this FRASA system by $\overline{\mathsf{S}}$. We define the stability of the FRASA system $\overline{\mathsf{S}}$ as follows.

Definition 1: The FRASA system $\overline{\mathsf{S}}$ is *stable* if for each link $n \in \mathcal{M}$, the number of packets in the corresponding transmitter, *i.e.*, the packets in the single buffer plus the

feedback loop, does not grow to infinity. Otherwise, $\overline{\mathsf{S}}$ is *unstable*.

Equivalently, since the number of packets in the single buffer must be finite, the stability of the feedback loop in each link determines the stability of the corresponding link in the FRASA system. Also, throughout this paper, we use the results from [16] to determine when a system is stable: on the assumption that the arrival and the service processes of a queue are stationary, the queue is stable if the average arrival rate is less than the average service rate, and the queue is unstable if the average arrival rate is larger than the average service rate.

When $\overline{\mathsf{S}}$ is stable, for each $n \in \mathcal{M}$, we have

$$\chi_n = \lambda_n + \chi_n(1-p_n) + \chi_n p_n \left[1 - \prod_{n' \in \mathcal{M}\setminus\{n\}} (1-\chi_{n'}p_{n'})\right]. \quad (1)$$

The second term on right hand side of (1) represents the arrival rate of the packets to the feedback loop due to the transmitter's decision of not transmitting the packet, while the third term on right hand side of (1) denotes the arrival rate of the packets to the feedback loop due to the transmitter's attempt to transmit the packet which results in a collision. When $\overline{\mathsf{S}}$ is stable, the arrival rate and the departure rate of the feedback loop are equal. Therefore, together with the arrival of new packets, the three terms on right hand side of (1) constitute the aggregate arrival rate χ_n. Simplifying (1), we get

$$\lambda_n = \chi_n p_n \prod_{n' \in \mathcal{M}\setminus\{n\}} (1-\chi_{n'}p_{n'}), \quad (2)$$

which states that when $\overline{\mathsf{S}}$ is stable, the loading supported by each link is equal to the successful transmission probability of the corresponding link. Since the feedback loop of each link is stable, we get for each $n \in \mathcal{M}$

$$\chi_n(1-p_n)+\chi_n p_n \left[1- \prod_{n' \in \mathcal{M}\setminus\{n\}} (1-\chi_{n'}p_{n'})\right] < 1-\lambda_n. \quad (3)$$

Substituting (2) into (3), we obtain $\chi_n < 1$. On the other hand, when $\overline{\mathsf{S}}$ is unstable, the feedback loop of at least one link, say link n, is unstable. Then the departure rate of the feedback loop of link n is $1-\lambda_n$. This implies that the aggregate arrival rate of link n is $\chi_n = \lambda_n + (1-\lambda_n) = 1$, which means that there is always a packet in the single buffer of the transmitter of link n. Therefore, we arrive at the following alternative definition of the stability of the FRASA system $\overline{\mathsf{S}}$.

Definition 2: The FRASA system $\overline{\mathsf{S}}$ is *stable* if for each $n \in \mathcal{M}$, $\chi_n < 1$. We define link n to be *infinitely backlogged* when $\chi_n = 1$. If $\overline{\mathsf{S}}$ contains at least one link with infinite backlog, $\overline{\mathsf{S}}$ is *unstable*.

To determine the stability region of a given FRASA system $\overline{\mathsf{S}}$, we first consider the *reduced FRASA system* $\overline{\mathsf{S}}_{\hat{n}}$ defined as follows. Assume the same arrival processes and transmission attempts in both systems, and both systems start with the same initial condition. In $\overline{\mathsf{S}}_{\hat{n}}$, when link $\hat{n}$ does not have any packet in its buffer and it decides to transmit, it will transmit a dummy packet, so that this link appears to have infinite-backlog, *i.e.*, $\chi_{\hat{n}} = 1$. The other links remain the same as in $\overline{\mathsf{S}}$. Hence, link $\hat{n}$ is active with probability $\chi_{\hat{n}}p_{\hat{n}} = p_{\hat{n}}$, while for $n \neq \hat{n}$, link n is active with probability $\chi_n p_n$. Therefore, $\overline{\boldsymbol{\lambda}} = \left(\overline{\lambda}_n\right)_{n\in\mathcal{M}}$, the successful transmission probability vector, is

$$\overline{\lambda}_n = \begin{cases} \chi_n p_n(1-p_{\hat{n}}) \displaystyle\prod_{n' \in \mathcal{M}\setminus\{n,\hat{n}\}} (1-\chi_{n'}p_{n'}), & n \neq \hat{n} \\ p_{\hat{n}} \displaystyle\prod_{n' \in \mathcal{M}\setminus\{\hat{n}\}} (1-\chi_{n'}p_{n'}), & n = \hat{n} \end{cases}, \quad (4)$$

with $\overline{\lambda}_{\hat{n}} > 0$. Then, $\lambda_n = \overline{\lambda}_n, \forall n \in \mathcal{M}$ is the *parametric form* of the boundary of the stability region of $\overline{\mathsf{S}}_{\hat{n}}$. We can obtain a non-parametric version by using (4) as follows.

Lemma 1: Consider $\overline{\mathsf{S}}_{\hat{n}}$. When

$$\frac{\lambda_{\hat{n}}(1-p_{\hat{n}})}{p_{\hat{n}}} \geq \frac{\lambda_n(1-p_n)}{p_n} \geq 0 \quad (5)$$

is satisfied for all $n \in \mathcal{M} \setminus \{\hat{n}\}$, the hypersurface $\mathsf{F}_{\hat{n}}$, *i.e.*,

$$\prod_{n' \in \mathcal{M}} [\lambda_{\hat{n}}(1-p_{\hat{n}}) + \lambda_{n'}p_{\hat{n}}] = p_{\hat{n}}[\lambda_{\hat{n}}(1-p_{\hat{n}})]^{M-1}, \quad (6)$$

is the *non-parametric form* of the boundary of the stability region of $\overline{\mathsf{S}}_{\hat{n}}$.

Proof: Refer to Appendix A. ∎

Recall the system is stable if all queues in the system are stable [5], [6], [8], and notice the expression $\frac{\lambda_n(1-p_n)}{p_n}$ in (5) is identical to the *instability rank* introduced in [6]. When $\max_{n\in\mathcal{M}} \frac{\lambda_n(1-p_n)}{p_n} = \frac{\lambda_{\hat{n}}(1-p_{\hat{n}})}{p_{\hat{n}}}$ holds as in (5), link $\hat{n}$ is the most probable one to be the first unstable link. Hence, we let link $\hat{n}$ to be infinitely backlogged and use Lemma 1 to obtain the stability region of FRASA as in the following Theorem.

Theorem 1: Let $\overline{\mathcal{R}}_{\hat{n}}$ be the set of arrival rate vectors $\boldsymbol{\lambda} = (\lambda_n)_{n\in\mathcal{M}}$ satisfying

$$\frac{\lambda_{\hat{n}}(1-p_{\hat{n}})}{p_{\hat{n}}} \geq \frac{\lambda_n(1-p_n)}{p_n} \geq 0, \forall n \in \mathcal{M} \setminus \{\hat{n}\}, \quad (7)$$

$$\prod_{n' \in \mathcal{M}} [\lambda_{\hat{n}}(1-p_{\hat{n}}) + \lambda_{n'}p_{\hat{n}}] < p_{\hat{n}}[\lambda_{\hat{n}}(1-p_{\hat{n}})]^{M-1}. \quad (8)$$

Then $\overline{\mathcal{R}} = \bigcup_{\hat{n}\in\mathcal{M}} \overline{R}_{\hat{n}}$ is the stability region of FRASA. The union here is actually a disjoint union.

Proof: Refer to Appendix B. ∎

We first illustrate our results for $M = 2$. When

$$\frac{\lambda_1(1-p_1)}{p_1} \geq \frac{\lambda_2(1-p_2)}{p_2} \geq 0$$

holds, the boundary of the stability region of FRASA is

$$\lambda_1[\lambda_1(1-p_1) + \lambda_2 p_1] = p_1\lambda_1(1-p_1),$$

which is reduced to

$$\lambda_1 = p_1\left(1 - \frac{\lambda_2}{1-p_1}\right)$$

after simplification. By symmetry, we also get

$$\lambda_2 = p_2\left(1 - \frac{\lambda_1}{1-p_2}\right)$$

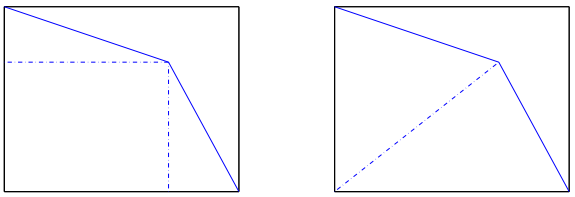

Fig. 2. Stability region with $M = 2$: (Upper) From [2]; (Lower) From FRASA.

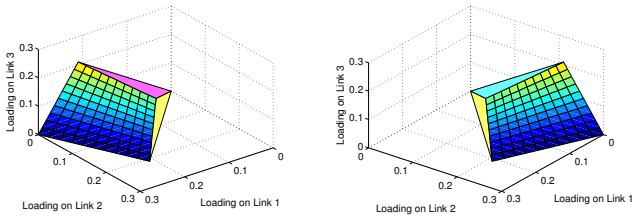

(a) $\overline{\mathcal{R}}_1$, stability region with link 1 having maximum instability rank.

(b) $\overline{\mathcal{R}}_2$, stability region with link 2 having maximum instability rank.

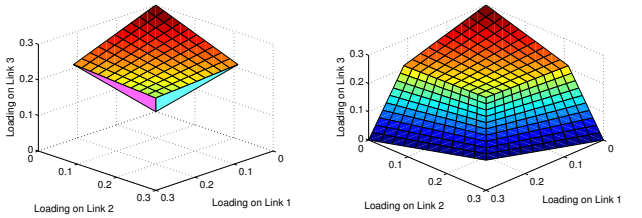

(c) $\overline{\mathcal{R}}_3$, stability region with link 3 having maximum instability rank.

(d) $\overline{\mathcal{R}}$, the whole stability region.

Fig. 3. Stability region of FRASA with $M = 3$ and transmission probabilities 0.3 by Lemma 1 and Theorem 1.

as the boundary of the stability region of FRASA when

$$\frac{\lambda_2(1-p_2)}{p_2} \geq \frac{\lambda_1(1-p_1)}{p_1} \geq 0$$

holds. The right part of Fig. 2 contains the final result of the stability region obtained from FRASA. The stability region derived in [2] is illustrated in the left part of Fig. 2 for comparison. We see that the final results are identical.

Next we consider the case of $M = 3$ and each link has a transmission probability of 0.3. Figs. 3(a), 3(b) and 3(c) illustrate the results of Lemma 1 for $\overline{\mathsf{S}}_1$, $\overline{\mathsf{S}}_2$ and $\overline{\mathsf{S}}_3$ respectively. The single-colored hyperplanes in Figs. 3(a), 3(b) and 3(c) form the partition of the positive orthant generated by (5), while the multi-colored hypersurfaces come from (6). The union of these regions constitutes the stability region in Fig. 3(d) as stated in Theorem 1.

IV. Validation of the FRASA Model

A. Simulation Results

In this section, we first use simulation to verify if FRASA is a good approximation to finite-user slotted ALOHA. Since when $M = 2$, we obtain identical results for both FRASA and finite-user slotted ALOHA, we consider $M = 3$ here.

Given any $\boldsymbol{p} = (p_1, p_2, p_3)$, to check whether the slotted ALOHA system with arrival rate vector $\boldsymbol{\lambda} = (\lambda_1, \lambda_2, \lambda_3)$ is

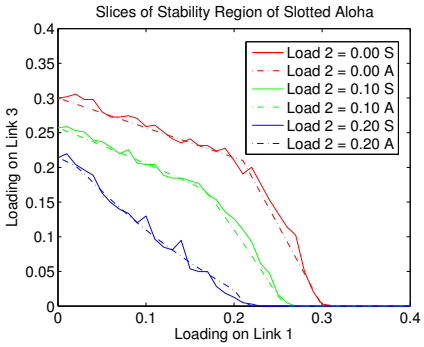

Fig. 4. Cross-section of stability region with $M = 3$, transmission probabilities 0.3 and λ_2 fixed.

stable or not by simulation, we extend the algorithm in [17]. For the w-th simulation run, we partition the simulation time into $\mathcal{N} \geq 2$ batches. For each queue n, we calculate its time-average queue length in each batch. Then we compute $\mathrm{Var}(\overline{Q}_{n,w})$, the sample variance of the time-average queue length, and $\hat{Q}_{n,w}$, the difference between the time-average queue length of the last and the second batch, and test the following hypothesis:

$$\frac{\hat{Q}_{n,w}}{\sqrt{2\mathrm{Var}(\overline{Q}_{n,w})}} > t_{1-\mathsf{a},\mathcal{N}-2}, \exists n \in \mathcal{M}, \tag{9}$$

where $t_{1-\mathsf{a},\mathcal{N}-2}$ is the $(1-\mathsf{a})$-percentile of t-distribution with $\mathcal{N}-2$ degrees of freedom. If (9) is satisfied, we assume the system is unstable; otherwise all queues in the slotted ALOHA system are stable and so is the system. If the system is unstable, there must exist $\hat{n} \in \mathcal{M}$ such that the length of queue $\hat{n}$ has positive linear growth rate, making (9) satisfied with high probability. Otherwise, the expectation of $\hat{Q}_{n,w}$ would be zero for all $n \in \mathcal{M}$, and with high probability (9) would be false. We perform $\mathcal{W}$ simulation runs and then use majority vote to determine whether the system is stable. To find the boundary of the stability region, for each λ_1 and λ_2, we use bisection method [18] to find λ_3 such that $\boldsymbol{\lambda}$ lies on the boundary.

For illustrative purposes, we only show the cross-sections of the stability regions. We let all links transmit with probability 0.3. In Fig. 4 we depict the cross-sections of the stability regions by fixing λ_2. The solid lines represent the simulation results while the dash-dot lines are obtained from FRASA. In general, there is a close match between the stability region of FRASA and the stability region of slotted ALOHA.

B. Comparison to Previous Bounds

Here, we demonstrate that FRASA is a good approximation to finite-user slotted ALOHA by showing the boundary values obtained from FRASA lie inside the upper and lower bounds in [6]. We fix the loadings on the first $M-1$ links, evaluate the "FRASA" value of λ_M, and the "Upper" and "Lower" bounds of λ_M by using Theorems 3 and 5 in [6] respectively. Before showing this, we point out that the bounds in [6] are applicable only when the instability rank assumption, *i.e.*, link M has the highest instability rank, holds. It is in general difficult to predict whether the instability rank assumption is valid or

TABLE I
COMPARISON FOR λ_M FOR $M = 3$ AND $p_1 = 0.6, p_2 = 0.7, p_3 = 0.8$.

	λ_1	λ_2	CHB	Upper	FRASA (Sim)	Lower
G1	0	0	0.8	0.8	0.8 (0.802)	0.8
	0	0.05	0.743	0.6	0.6 (0.601)	0.6
	0.03	0	0.76	0.68	0.68 (0.683)	0.68
G2	0.018	0.028	0.744	0.616	0.603 (0.594)	0.508
G3	0.03	0.05	0.703	0.48	0.423 (0.375)	0.24
G4	0.035	0.0561*	0.689	0.436	0.344 (0.204)	0.115
	0.025	0.0563*	0.702	0.475	0.421 (0.360)	0.278

TABLE II
COMPARISON FOR λ_M FOR $M = 3$ AND $p_1 = 0.1, p_2 = 0.1, p_3 = 0.1$.
(NOTE: [6]'S BOUND IS NOT APPLICABLE FOR THE EXAMPLE IN G4)

	λ_1	λ_2	CHB	Upper	FRASA (Sim)	Lower
G1	0	0	0.1	0.1	0.1 (0.100)	0.1
	0	0.03	0.097	0.097	0.097 (0.097)	0.097
G2	0.04	0.04	0.091	0.091	0.091 (0.091)	0.091
G3	0.078	0.078	0.082	0.083	0.082 (0.082)	0.082
G4	0.078	0.082*	0.076	0.082	0.076 (0.077)	0.081

not, in particular when there are some λ_n satisfying $\lambda_n > p_n \prod_{n' \in \mathcal{M}\setminus\{n\}} \overline{p}_{n'}$. However, such restriction does not exist in computing the "FRASA" value of λ_M. We first let link M be the link with the highest instability rank, *i.e.*, $\hat{n} = M$. Then we solve (6) for λ_M, which is an equation of degree $M-1$, and get $M-1$ values of λ_M. Exactly one of them is the desired value, which makes the instability rank of link M the highest. Otherwise, we find the link with the highest instability rank among the first $M-1$ links. We let it equal $\hat{n}$ and solve (6) for λ_M, which is an equation of degree one. In this case, we get a nonnegative value which is the desired value of λ_M. Otherwise, we conclude that with the loadings on the first $M-1$ links, it is impossible to keep the system stable no matter how small λ_M is.

We consider the numerical examples in [2] and [6]. Some of the examples are reproduced in Tables I- VI. More numerical results are included in [19]. The loadings are classified into four groups in each table. In G1, one or more λ_n are zero. In G2, all λ_n are approximately equal to $\frac{1}{2}p_n \prod_{n' \in \mathcal{M}\setminus\{n\}} \overline{p}_{n'}$. In G3, all λ_n are close to $p_n \prod_{n' \in \mathcal{M}\setminus\{n\}} \overline{p}_{n'}$. In G4, one or more λ_n satisfy $\lambda_n > p_n \prod_{n' \in \mathcal{M}\setminus\{n\}} \overline{p}_{n'}$, and these λ_n are marked with asterisks in the tables. In all cases, the values predicted from FRASA lie inside the upper and lower bounds in [6]. Simulation results are shown in brackets in the tables. While the difference between the simulation result and the corresponding "FRASA" value can be as large as 40% (the first case of G4 in Table I), for most cases the simulation results deviate from the corresponding "FRASA" values by at most $\pm 2\%$. The examples also show that the bounds in [6] may not be always applicable, as in the case of G4 in Table II.

For the first case of G4 in Table I, we plot the contour of the stability region of FRASA in Fig. 5 to investigate the reason for such a large discrepancy between the stability regions of slotted ALOHA and FRASA. This contour plot shows that when $\lambda_1 = 0.035$ and $\lambda_2 = 0.0561$, the contour lines are very close together, so the boundary is very sensitive to small changes in λ_1 and λ_2. Therefore, it is difficult to obtain the boundary of the stability region of slotted ALOHA by simulations.

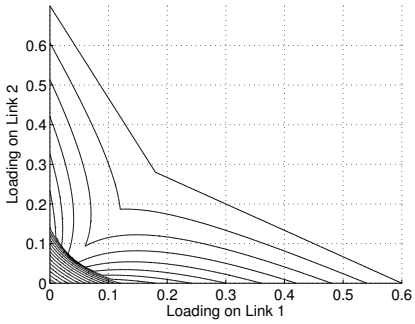

Fig. 5. Contour plot of the stability region of FRASA for the first case of G4 in Table I.

V. CONVEX HULL BOUND

Although Theorem 1 gives us a closed-form expression for the stability region of FRASA, this stability region is not convex when $M > 2$ (as shown in the next section). Therefore we are motivated to derive outer and inner bounds on the stability region of FRASA that are convex and piecewise linear, which can be used to find the upper and lower bounds on network capacity respectively. In this section, we develop a convex and piecewise linear outer bound on the stability region of FRASA by using *corner points* of the stability region of FRASA. For each $\mathcal{M}' \subseteq \mathcal{M}$, we obtain a corner point $\Pi^{\mathsf{p}^{\mathcal{M}}(\mathcal{M}')} = \left(\Pi_n^{\mathsf{p}^{\mathcal{M}}(\mathcal{M}')}\right)_{n\in\mathcal{M}}$, where

$$\Pi_n^{\mathsf{p}^{\mathcal{M}}(\mathcal{M}')} = \begin{cases} p_n \prod_{n' \in \mathcal{M}'\setminus\{n\}} \overline{p}_{n'}, & n \in \mathcal{M}' \\ 0, & n \in \mathcal{M}\setminus\mathcal{M}' \end{cases}. \quad (10)$$

These corner points, by construction, lie on the boundary of the stability region of FRASA because they satisfy the parametric form (4). The following Lemma states the relationship between the boundary of the stability region of FRASA and the corner points.

Lemma 2: The boundary of the stability region of $\overline{\mathsf{S}}_{\hat{n}}$, *i.e.*, the hypersurface $\mathsf{F}_{\hat{n}}$, is contained in the convex hull $\mathsf{H}_{\hat{n}}$ generated by the corner points $\Pi^{\mathsf{p}^{\mathcal{M}}(\mathcal{M}'\cup\{\hat{n}\})}$ for all $\mathcal{M}' \subseteq \mathcal{M}\setminus\{\hat{n}\}$, *i.e.*, every point satisfying (6) is a convex combination of the corner points $\Pi^{\mathsf{p}^{\mathcal{M}}(\mathcal{M}'\cup\{\hat{n}\})}$ for all $\mathcal{M}' \subseteq \mathcal{M}\setminus\{\hat{n}\}$.

Proof: Refer to Appendix C. ∎

By using Lemma 2 and Theorem 1, we obtain the following Theorems about using convex hulls to bound the stability region of FRASA. These bounds can be computed using the transmission probability vector only.

Theorem 2 (Bound of Convex-Hull Union): The convex hull generated by $\Pi^{\mathsf{p}^{\mathcal{M}}(\mathcal{M}'\cup\{\hat{n}\})}$ for all $\mathcal{M}' \subseteq \mathcal{M}\setminus\{\hat{n}\}$ together with $\mathbf{0}$, *i.e.*, the origin, is a piecewise linear outer bound on $\overline{\mathcal{R}}_{\hat{n}}$. Denote this convex hull by $\mathcal{H}_{\hat{n}}$. Therefore, the union of these $\mathcal{H}_{\hat{n}}$ for all $\hat{n} \in \mathcal{M}$, *i.e.*, $\overline{\mathcal{H}} = \bigcup_{\hat{n}\in\mathcal{M}} \mathcal{H}_{\hat{n}}$,

TABLE III
COMPARISON FOR λ_M FOR $M = 5$ AND $p_1 = p_2 = p_3 = p_4 = p_5 = 0.5$.

	λ_1	λ_2	λ_3	λ_4	CHB	Upper	FRASA (Sim)	Lower
G1	0	0	0	0	0.5	0.5	0.5 (0.500)	0.5
	0	0	0	0.015	0.485	0.485	0.485 (0.487)	0.485
	0	0	0.015	0.015	0.47	0.47	0.470 (0.469)	0.462
	0	0.015	0.015	0.015	0.455	0.455	0.453 (0.455)	0.422
G2	0.015	0.015	0.015	0.015	0.44	0.44	0.437 (0.433)	0.337
G3	0.03	0.03	0.03	0.03	0.38	0.38	0.364 (0.348)	0.048
G4	0.03	0.03	0.03	0.033*	0.377	0.377	0.360 (0.344)	0.046
	0.033*	0.032*	0.031	0.03	0.374	0.374	0.356 (0.330)	0.039
	0.0325*	0.032*	0.0315*	0.03	0.374	0.374	0.356 (0.329)	0.038

TABLE IV
COMPARISON FOR λ_M FOR $M = 5$ AND $p_1 = 0.4, p_2 = 0.5, p_3 = 0.6, p_4 = 0.7, p_5 = 0.8$.

	λ_1	λ_2	λ_3	λ_4	CHB	Upper	FRASA (Sim)	Lower
G1	0	0	0	0	0.8	0.8	0.8 (0.802)	0.8
	0	0	0	0.005	0.794	0.78	0.78 (0.782)	0.78
	0	0	0.005	0.005	0.788	0.76	0.759 (0.761)	0.744
	0	0.005	0.005	0.005	0.780	0.74	0.738 (0.737)	0.686
G2	0.002	0.003	0.005	0.005	0.780	0.74	0.738 (0.731)	0.629
G3	0.004	0.006	0.01	0.01	0.759	0.68	0.672 (0.664)	0.409
G4	0.004	0.006	0.01	0.017*	0.751	0.652	0.640 (0.626)	0.173
	0.004	0.006	0.011*	0.017*	0.750	0.648	0.635 (0.617)	0.152
	0.002	0.0073*	0.011*	0.017*	0.751	0.651	0.639 (0.621)	0.312

TABLE V
COMPARISON FOR λ_M FOR $M = 10$ AND $p_1 = p_2 = p_3 = 0.1, p_4 = 0.2, p_5 = 0.3, p_6 = 0.4, p_7 = 0.5, p_8 = 0.6, p_9 = 0.7, p_{10} = 0.8$.

	λ_1 $\times 10^{-3}$	λ_2, λ_3 $\times 10^{-3}$	λ_4 $\times 10^{-3}$	λ_5 $\times 10^{-3}$	λ_6 $\times 10^{-3}$	λ_7 $\times 10^{-3}$	λ_8 $\times 10^{-3}$	λ_9 $\times 10^{-3}$	Upper	FRASA (Sim)	Lower
G1	0	0	0	0	0	0	0	0	0.8	0.8 (0.801)	0.8
	0	0.15	0.35	0.5	0.5	1	2	3	0.769	0.769 (0.766)	0.654
G2	0.15	0.15	0.35	0.5	0.5	1	2	3	0.769	0.768 (0.768)	0.637
G3	0.3	0.3	0.7	1	1	2	4	6	0.738	0.736 (0.735)	0.412
G4	0.3	0.3	0.7	1	1	2	4	6.86*	0.734	0.732 (0.731)	0.402
	0.01	0.327*	0.735*	1.26*	1.96*	2.94*	4.41*	6.86*	0.725	0.722 (0.719)	0.041

TABLE VI
COMPARISON FOR λ_M FOR $M = 10$ AND $p_1 = p_2 = p_3 = p_4 = p_5 = p_6 = p_7 = p_8 = p_9 = p_{10} = 0.1$.

	λ_1	λ_2,λ_3,λ_4	λ_5,λ_6,λ_7,λ_8,λ_9	Upper	FRASA (Sim)	Lower
G1	0	0	0	0.1	0.1 (0.100)	0.1
	0	0.019	0.019	0.083	0.081 (0.082)	0.077
G2	0.019	0.019	0.019	0.081	0.079 (0.079)	0.073
G3	0.036	0.036	0.036	0.064	0.050 (0.050)	0.043
G4	0.039*	0.036	0.036	0.064	0.049 (0.049)	0.043
	0.039*	0.039*	0.036	0.063	0.046 (0.046)	0.041

is a piecewise linear outer bound on the stability region of FRASA. The union here is also disjoint.

Proof: Refer to Appendix D. ∎

Theorem 3 (Convex Hull Bound): $\mathcal{H}$, the convex hull generated by $\Pi^{\mathrm{p}^{\mathcal{M}}(\mathcal{M}')}$ for all $\mathcal{M}' \subseteq \mathcal{M}$, is a convex and piecewise linear outer bound on the stability region of FRASA.

Proof: Refer to Appendix E. ∎

In finding the bounds on λ_M given the loadings on the other links, we do not have to rely on the instability rank assumption as in [6]. To apply Theorem 2, we first assume link M to have the highest instability rank, and generate the corresponding convex hull. If the assumption is valid, we can find a lower bound and an upper bound from the convex hull. Otherwise, we choose from the remaining links the link with the highest instability rank and repeat the process. Theorem 3 can be applied in any case in finding the upper bound.

As an example, assuming the transmission probabilities of all links are 0.3, Figs. 6(a), 6(b) and 6(c) show the convex hulls $\mathcal{H}_1$, $\mathcal{H}_2$ and $\mathcal{H}_3$ respectively. Fig. 6(d) shows $\overline{\mathcal{H}}$, the union of the convex hulls in Figs. 6(a), 6(b) and 6(c). Fig. 6(e) depicts $\mathcal{H}$, the convex hull generated by all corner points. The polytopes in Figs. 6(d) and 6(e) are identical. To show that this is not necessarily true, we give another example in which the transmission probabilities of all links are 0.6. In this example, $\overline{\mathcal{H}}$ in Fig. 7(d) is contained inside $\mathcal{H}$ in Fig. 7(e).

VI. $\boldsymbol{p}$-CONVEXITY

The examples in previous section show that the bounds on the stability region of FRASA obtained from Theorems 2 and 3, *i.e.*, $\overline{\mathcal{H}}$ and $\mathcal{H}$ respectively, need not be identical. Intuitively, for $\overline{\mathcal{H}} = \mathcal{H}$, we require $\overline{\mathcal{H}}$ to be convex, which means the transmission probability vector may need to satisfy

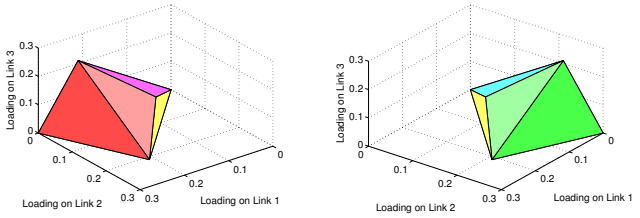

(a) $\mathcal{H}_1$, convex hull of $\overline{\mathcal{R}}_1$. (b) $\mathcal{H}_2$, convex hull of $\overline{\mathcal{R}}_2$.

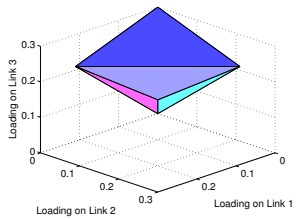

(c) $\mathcal{H}_3$, convex hull of $\overline{\mathcal{R}}_3$.

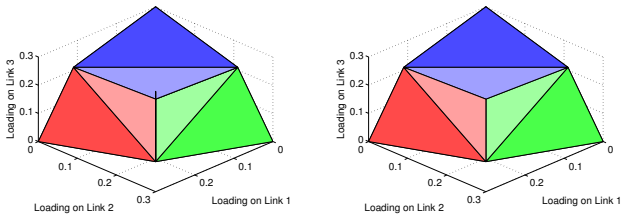

(d) $\overline{\mathcal{H}}$, bound of convex-hull union. (e) $\mathcal{H}$, convex hull bound.

Fig. 6. Convex hull bound on the stability region of FRASA with $M = 3$ and transmission probabilities 0.3 by Theorems 2 and 3.

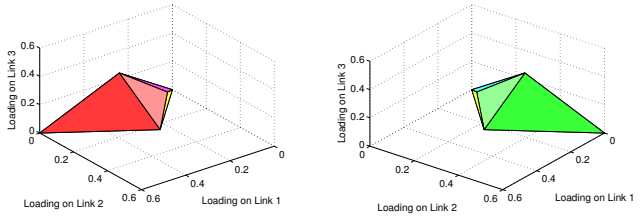

(a) $\mathcal{H}_1$, convex hull of $\overline{\mathcal{R}}_1$. (b) $\mathcal{H}_2$, convex hull of $\overline{\mathcal{R}}_2$.

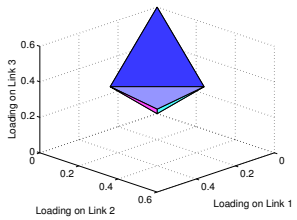

(c) $\mathcal{H}_3$, convex hull of $\overline{\mathcal{R}}_3$.

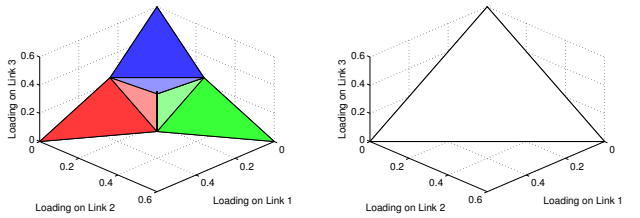

(d) $\overline{\mathcal{H}}$, bound of convex-hull union. (e) $\mathcal{H}$, convex hull bound.

Fig. 7. Convex hull bound on the stability region of FRASA with $M = 3$ and transmission probabilities 0.6 by Theorems 2 and 3.

some "convexity" conditions. We formalize these ideas and investigate the necessary and sufficient condition for $\overline{\mathcal{H}}$ and $\mathcal{H}$ to be identical.

We first define $\boldsymbol{p}$-convexity, and characterize the condition on the transmission probability vector for $\boldsymbol{p}$-convexity to hold.

Definition 3: We use the corner points $\Pi^{\mathsf{p}^{\mathcal{M}}(\mathcal{M}\setminus\{\bar{n}\})}$ for each $\bar{n} \in \mathcal{M}$ to form a hyperplane $\Omega^{\mathcal{M}}$. If the corner points $\Pi^{\mathsf{p}^{\mathcal{M}}(\mathcal{M})}$ and $\mathbf{0}$ lie on opposite sides of $\Omega^{\mathcal{M}}$, or $\Pi^{\mathsf{p}^{\mathcal{M}}(\mathcal{M})}$ lies on $\Omega^{\mathcal{M}}$, the stability region of FRASA is said to be $\boldsymbol{p}$-*convex*.

Theorem 4: The stability region of FRASA is $\boldsymbol{p}$-convex if and only if

$$\sum_{n\in\mathcal{M}} p_n \leq 1. \tag{11}$$

Proof: Refer to Appendix F. ∎

The $\boldsymbol{p}$-convexity of the stability region of FRASA can be regarded as a measure of contention level in the system. p_n can be viewed as the proportion of time that link n is active. $\sum_{n\in\mathcal{M}} p_n \leq 1$ represents the case that the increase in channel utilization outweighs the increase in contention due to addition of one more link to the system. This is possible because when the channel utilization is small, the probability that a new link chooses an idle time slot to transmit is large, therefore the contention introduced by this new link is small and the stability region of FRASA is $\boldsymbol{p}$-convex. On the other hand, if $\sum_{n\in\mathcal{M}} p_n > 1$, the contention level is so large that it is not beneficial to introduce one more link to the system. Even in the ideal case, *i.e.*, TDMA with perfect scheduling, it is impossible to assign time slots to the links such that there is no contention. Hence, contention is inevitable, and the stability region of FRASA is not $\boldsymbol{p}$-convex. Consequently, it is undesirable to allow the links to be active with transmission probability vector $(p_n)_{n\in\mathcal{M}}$.

We now give a necessary and sufficient condition for the equality of $\overline{\mathcal{H}}$ and $\mathcal{H}$.

Theorem 5: $\overline{\mathcal{H}} = \mathcal{H}$ if and only if the stability region of FRASA is $\boldsymbol{p}$-convex.

Proof: Refer to Appendix G. ∎

From Theorem 4, we know that (11) guarantees the stability region of FRASA to be $\boldsymbol{p}$-convex. Then, can (11) assure the convexity of the stability region of FRASA? Recall Theorem 1 that the boundary of the stability region of FRASA consists of M hypersurfaces, *i.e.*, $\mathsf{F}_{\hat{n}}$ for all $\hat{n} \in \mathcal{M}$. Also, Lemma 2 says that for each $\hat{n} \in \mathcal{M}$, the hypersurface $\mathsf{F}_{\hat{n}}$ is contained inside the convex hull $\mathsf{H}_{\hat{n}}$. If (11) holds, we need an additional condition to guarantee the convexity of the stability region of FRASA: for all $\hat{n} \in \mathcal{M}$, $\mathsf{F}_{\hat{n}}$ is a hyperplane, meaning that $\mathsf{F}_{\hat{n}} = \mathsf{H}_{\hat{n}}$. This additional condition is satisfied when $M = 2$ as illustrated in Section III. Therefore, for $M = 2$, $\boldsymbol{p}$-convexity is equivalent to convexity and (11) guarantees the convexity of the stability region of FRASA. However, this is not the case for $M > 2$ since if such a hyperplane exists for some $\hat{n}$, the boundary of the stability region of FRASA is linear in $\lambda_{\hat{n}}$, contradicting to the non-parametric form (6) that the boundary is of degree at least two in $\lambda_{\hat{n}}$ when $M > 2$. Hence, the nonconvexity of the stability region of FRASA when $M > 2$

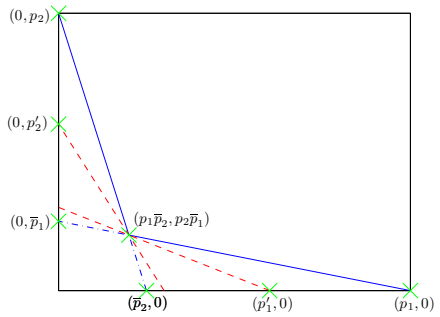

Fig. 8. Supporting hyperplane bound.

follows.

Consider again the examples in Figs. 6 and 7. In Fig. 6, $\sum_{n\in\mathcal{M}} p_n = 0.9 \leq 1$, therefore the stability region is $\boldsymbol{p}$-convex and $\overline{\mathcal{H}} = \mathcal{H}$. On the other hand, in Fig. 7, $\sum_{n\in\mathcal{M}} p_n = 1.8 > 1$, and $\overline{\mathcal{H}} \subsetneq \mathcal{H}$. In other words, the convex hull bound is tighter if and only if the stability region is $\boldsymbol{p}$-convex.

To illustrate the importance of $\boldsymbol{p}$-convexity, we also compute the "CHB" value, *i.e.*, the upper bound from Theorem 3, in Tables I- IV. When the stability region of FRASA is $\boldsymbol{p}$-convex, the convex hull bound is tighter than the bound given by [6]. Otherwise, the convex hull bound is loose, which demonstrates the tradeoff between the convexity and the tightness of the bounds.

VII. Supporting Hyperplane Bound

In this section, we give a convex and piecewise linear inner bound on the stability region of FRASA by using *supporting hyperplanes*. A supporting hyperplane of a convex set is a hyperplane such that it intersects with the convex set and the convex set entirely belongs to only one of the closed half spaces generated by the hyperplane. This inner bound is obtained based on the result of Lemma 2.

Theorem 6 (Supporting Hyperplane Bound): For each $\hat{n} \in \mathcal{M}$, we construct a supporting hyperplane $\mathsf{P}_{\hat{n}}$ which supports the convex hull $\mathsf{H}_{\hat{n}}$ in Lemma 2 at $\Pi^{\mathbf{p}^{\mathcal{M}}(\mathcal{M})}$ such that

1) it lies below $\mathsf{H}_{\hat{n}}$; and
2) it has positive intercepts on all coordinate axes.

We let $\mathcal{S}_{\hat{n}}$ be the closed half space below $\mathsf{P}_{\hat{n}}$. Then the intersection of all these half spaces in the positive orthant, *i.e.*, $\mathcal{S} = \bigcap_{\hat{n}\in\mathcal{M}} \mathcal{S}_{\hat{n}} \cap \{\boldsymbol{\lambda}\colon \lambda_n \geq 0, \forall n \in \mathcal{M}\}$, is a convex and piecewise linear inner bound on the stability region of FRASA.

Proof: Refer to Appendix H. ∎

Consider Fig. 8 where $M = 2$. The hyperplane P_1 can be any line passing through $(p_1', 0)$ and $(p_1\overline{p}_2, p_2\overline{p}_1)$, where $p_1\overline{p}_2 \leq p_1' \leq p_1$. The hyperplane P_2 can be found similarly. These hyperplanes are shown as the red dashed lines in Fig. 8. The intersection of the closed half spaces below the red lines in the positive quadrant is the inner bound from Theorem 6.

This supporting hyperplane bound is arbitrary, in the sense that for each $\hat{n} \in \mathcal{M}$, as long as the hyperplane constructed satisfies the requirements listed, $\mathcal{S}$ will be an inner bound. If we require the inner bound to occupy the maximum hypervolume, then this problem is equivalent to finding a maximum-hypervolume convex subset of the stability region of FRASA. To the best of our knowledge, this is studied only for $M = 2$ [20]. In this case, the problem is to find the maximum-area convex subset of a polygon. First we consider the case that $p_1 + p_2 > 1$, *i.e.*, the stability region of FRASA is not $\boldsymbol{p}$-convex. By calculus, the maximum-hypervolume convex subset is either the triangle between the vertices $(p_1, 0)$, $(0, \overline{p}_1)$ and $\mathbf{0}$, or the triangle between the vertices $(0, p_2)$, $(\overline{p}_2, 0)$ and $\mathbf{0}$. In either cases, the supporting hyperplanes we need in Theorem 6 coincide. This is a special case of the result in [20]. On the other hand, if the stability region of FRASA is $\boldsymbol{p}$-convex, *i.e.*, $p_1 + p_2 \leq 1$, the stability region itself is the maximum-hypervolume convex subset, since $\boldsymbol{p}$-convexity is equivalent to convexity as stated in previous section. In this case, the line segments of the boundary are already the supporting hyperplanes we need.

VIII. Conclusion

In this paper, we proposed FRASA, Feedback Retransmission Approximation for Slotted ALOHA, to serve as a surrogate to approximate finite-user slotted ALOHA. From FRASA, we obtained in closed form the exact stability region for any number of users in the system under the collision channel. We illustrated that the result from FRASA is identical to the analytical result of finite-user slotted ALOHA when there are two users. Simulation showed that the stability region obtained from FRASA is a good approximation to the stability region of finite-user slotted ALOHA. We demonstrated that our results from FRASA has a wider range of applicability than the existing bounds. We also established a convex hull bound, which is convex, piecewise linear and outer-bounds the stability region of FRASA. This convex hull bound can be generated by using the transmission probability vector only. We introduced $\boldsymbol{p}$-convexity, which is essential to ensure the convex hull bound to be close to the boundary of the stability region of FRASA. From these results, we deduced that the stability region of FRASA is nonconvex when there are more than two users. A separate convex and piecewise linear inner bound, supporting hyperplane bound, was also introduced.

Appendix A
Proof of Lemma 1

Starting from the parametric form (4), for $n \in \mathcal{M} \setminus \{\hat{n}\}$,

$$\frac{\lambda_n}{\lambda_{\hat{n}}} = \frac{\chi_n p_n (1-p_{\hat{n}}) \prod_{n'\in\mathcal{M}\setminus\{n,\hat{n}\}} (1-\chi_{n'}p_{n'})}{p_{\hat{n}} \prod_{n'\in\mathcal{M}\setminus\{\hat{n}\}} (1-\chi_{n'}p_{n'})} = \frac{\chi_n p_n (1-p_{\hat{n}})}{p_{\hat{n}}(1-\chi_n p_n)}.$$

Therefore,

$$\chi_n = \frac{\lambda_n p_{\hat{n}}}{\lambda_{\hat{n}}(1-p_{\hat{n}})p_n + \lambda_n p_{\hat{n}} p_n}$$

and the condition $0 \le \chi_n \le 1$ is translated into

$$\frac{\lambda_{\hat{n}}(1-p_{\hat{n}})}{p_{\hat{n}}} \ge \frac{\lambda_n(1-p_n)}{p_n} \ge 0.$$

Combining these results,

$$\begin{aligned}\lambda_{\hat{n}} &= p_{\hat{n}} \prod_{n' \in \mathcal{M}\setminus\{\hat{n}\}} (1-\chi_{n'}p_{n'}) \\ &= p_{\hat{n}} \prod_{n' \in \mathcal{M}\setminus\{\hat{n}\}} \left[1 - \frac{\lambda_{n'}p_{\hat{n}}p_{n'}}{\lambda_{\hat{n}}(1-p_{\hat{n}})p_{n'} + \lambda_{n'}p_{\hat{n}}p_{n'}}\right] \\ &= p_{\hat{n}} \prod_{n' \in \mathcal{M}\setminus\{\hat{n}\}} \frac{\lambda_{\hat{n}}(1-p_{\hat{n}})}{\lambda_{\hat{n}}(1-p_{\hat{n}}) + \lambda_{n'}p_{\hat{n}}},\end{aligned}$$

we obtain

$$\prod_{n' \in \mathcal{M}} [\lambda_{\hat{n}}(1-p_{\hat{n}}) + \lambda_{n'}p_{\hat{n}}] = p_{\hat{n}}[\lambda_{\hat{n}}(1-p_{\hat{n}})]^{M-1}$$

as the boundary of the stability region of $\overline{\mathsf{S}}_{\hat{n}}$. ■

APPENDIX B
PROOF OF THEOREM 1

By (7), the positive orthant is partitioned into M regions. In the region that $\max_{n\in\mathcal{M}} \frac{\lambda_n(1-p_n)}{p_n} = \frac{\lambda_{\hat{n}}(1-p_{\hat{n}})}{p_{\hat{n}}}$, *i.e.*, (7) holds, Lemma 1 gives the stability region of the reduced FRASA system $\overline{\mathsf{S}}_{\hat{n}}$, which is

$$\prod_{n' \in \mathcal{M}} [\lambda_{\hat{n}}(1-p_{\hat{n}}) + \lambda_{n'}p_{\hat{n}}] < p_{\hat{n}}[\lambda_{\hat{n}}(1-p_{\hat{n}})]^{M-1}.$$

We will show that this is also the stability region of the FRASA system $\overline{\mathsf{S}}$ when (7) holds.

First we show that the stability region of $\overline{\mathsf{S}}_{\hat{n}}$ is an inner bound on the stability region of $\overline{\mathsf{S}}$. Observe that the introduction of dummy packets on link $\hat{n}$ in $\overline{\mathsf{S}}_{\hat{n}}$ does not decrease the queue size of link $\hat{n}$, and it does not decrease the queue size of link $n \in \mathcal{M}\setminus\{\hat{n}\}$ because these dummy packets introduce additional interference to other links. Hence, the queue sizes of $\overline{\mathsf{S}}_{\hat{n}}$ stochastically dominate the queue sizes of $\overline{\mathsf{S}}$. Therefore, stability of the reduced FRASA system implies stability of the FRASA system.

Next we show that the stability region of $\overline{\mathsf{S}}_{\hat{n}}$ is an outer bound on the stability region of $\overline{\mathsf{S}}$. This follows from the indistinguishability argument used in [2], [8]. If link $\hat{n}$ in $\overline{\mathsf{S}}_{\hat{n}}$ is unstable, then the queue size of link $\hat{n}$ grows to infinity without emptying with nonzero probability. As long as this queue does not empty, both systems are indistinguishable (conditioned on that both systems start with the same initial condition and have the same arrival processes and transmission attempts), in the sense that the packets transmitted on link $\hat{n}$ are always real packets. Therefore the same evolution of the queue process happens in both systems, and $\overline{\mathsf{S}}$ is unstable as well.

Thus, the region formed by (7) and (8) is part of the stability region of $\overline{\mathsf{S}}$ when (7) holds. By taking the union over all $\hat{n}$, we obtain the stability region of FRASA. ■

APPENDIX C
PROOF OF LEMMA 2

Let $\Pi = (\Pi_n)_{n\in\mathcal{M}}$ be a point satisfying (6). Then, from the parametric form (4),

$$\Pi_n = \begin{cases} \chi_n p_n(1-p_{\hat{n}}) \displaystyle\prod_{n' \in \mathcal{M}\setminus\{n,\hat{n}\}} (1-\chi_{n'}p_{n'}), & n \ne \hat{n} \\ p_{\hat{n}} \displaystyle\prod_{n' \in \mathcal{M}\setminus\{\hat{n}\}} (1-\chi_{n'}p_{n'}), & n = \hat{n} \end{cases}. \tag{12}$$

If Π is a convex combination of $\Pi^{\mathsf{p}^{\mathcal{M}}(\mathcal{M}'\cup\{\hat{n}\})}$ for all $\mathcal{M}' \subseteq \mathcal{M}\setminus\{\hat{n}\}$, then

$$\Pi_n = \begin{cases} p_n\overline{p}_{\hat{n}} \displaystyle\sum_{\mathcal{M}':\, n\in\mathcal{M}'\subseteq\mathcal{M}\setminus\{\hat{n}\}} \phi_{\mathcal{M}'} \prod_{n' \in \mathcal{M}'\setminus\{n\}} \overline{p}_{n'}, & n \ne \hat{n} \\ p_{\hat{n}} \displaystyle\sum_{\mathcal{M}'\subseteq\mathcal{M}\setminus\{\hat{n}\}} \phi_{\mathcal{M}'} \prod_{n' \in \mathcal{M}'} \overline{p}_{n'}, & n = \hat{n} \end{cases} \tag{13}$$

where

$$\sum_{\mathcal{M}'\subseteq\mathcal{M}\setminus\{\hat{n}\}} \phi_{\mathcal{M}'} = 1 \text{ and } \phi_{\mathcal{M}'} \ge 0, \forall \mathcal{M}' \subseteq \mathcal{M}\setminus\{\hat{n}\}.$$

We will show that $\{\phi_{\mathcal{M}'}\}_{\mathcal{M}'\subseteq\mathcal{M}\setminus\{\hat{n}\}}$ always exists. When $n = \hat{n}$, we get

$$\sum_{\mathcal{M}'\subseteq\mathcal{M}\setminus\{\hat{n}\}} \phi_{\mathcal{M}'} \prod_{n' \in \mathcal{M}'} \overline{p}_{n'} = \prod_{n' \in \mathcal{M}\setminus\{\hat{n}\}} (1-\chi_{n'}p_{n'}).$$

Consider this as a multinomial in $\{p_n\}_{n\in\mathcal{M}\setminus\{\hat{n}\}}$. By equating the coefficient of $\prod_{n' \in \mathcal{M}''} p_{n'}$ for all $\mathcal{M}'' \subseteq \mathcal{M}\setminus\{\hat{n}\}$, we get

$$\sum_{\mathcal{M}':\, \mathcal{M}''\subseteq\mathcal{M}'\subseteq\mathcal{M}\setminus\{\hat{n}\}} \phi_{\mathcal{M}'} = \prod_{n' \in \mathcal{M}''} \chi_{n'}. \tag{14}$$

Also by equating the coefficient of $\prod_{n' \in \mathcal{M}''} p_{n'}$ for all $\mathcal{M}'' \subseteq \mathcal{M}\setminus\{n,\hat{n}\}$ with $n \ne \hat{n}$, we get

$$\sum_{\mathcal{M}':\, \mathcal{M}''\cup\{n\}\subseteq\mathcal{M}'\subseteq\mathcal{M}\setminus\{\hat{n}\}} \phi_{\mathcal{M}'} = \chi_n \prod_{n' \in \mathcal{M}''} \chi_{n'}.$$

Observe that this is only a special case of (14), it suffices to consider (14) only. Notice that (14) is a system of linear equations. By Gaussian elimination, we see that for all $\mathcal{M}'' \subseteq \mathcal{M}\setminus\{\hat{n}\}$,

$$\begin{aligned}\phi_{\mathcal{M}''} &= \sum_{\mathcal{M}':\, \mathcal{M}''\subseteq\mathcal{M}'\subseteq\mathcal{M}\setminus\{\hat{n}\}} (-1)^{|\mathcal{M}'|-|\mathcal{M}''|} \prod_{n' \in \mathcal{M}'} \chi_{n'} \\ &= \prod_{n' \in \mathcal{M}''} \chi_{n'} \prod_{n'' \in \mathcal{M}\setminus(\mathcal{M}''\cup\{\hat{n}\})} (1-\chi_{n''}) \ge 0.\end{aligned}$$

Also, by considering $\mathcal{M}'' = \emptyset$ in (14), we obtain

$$\sum_{\mathcal{M}'\subseteq\mathcal{M}\setminus\{\hat{n}\}} \phi_{\mathcal{M}'} = 1.$$

Therefore, every point satisfying (6) is a convex combination of $\Pi^{\mathsf{p}^{\mathcal{M}}(\mathcal{M}'\cup\{\hat{n}\})}$ for all $\mathcal{M}' \subseteq \mathcal{M}\setminus\{\hat{n}\}$. ■

APPENDIX D
PROOF OF THEOREM 2

Consider the reduced FRASA system $\overline{\mathsf{S}}_{\hat{n}}$ and let $\mathcal{M}' \subseteq \mathcal{M} \setminus \{\hat{n}\}$. From (10), for every $n \in \mathcal{M} \setminus \{\hat{n}\}$, all corner points $\Pi^{\mathsf{p}^{\mathcal{M}}(\mathcal{M}' \cup \{\hat{n}\})}$ with $n \in \mathcal{M}'$ and $\mathbf{0}$ lie on the boundary $\frac{\lambda_{\hat{n}}(1-p_{\hat{n}})}{p_{\hat{n}}} = \frac{\lambda_n(1-p_n)}{p_n}$, all corner points $\Pi^{\mathsf{p}^{\mathcal{M}}(\mathcal{M}' \cup \{\hat{n}\})}$ with $n \notin \mathcal{M}' \cup \{\hat{n}\}$ and $\mathbf{0}$ lie on the boundary $\frac{\lambda_n(1-p_n)}{p_n} = 0$. Also, for all $n \in \mathcal{M} \setminus \{\hat{n}\}$, the condition $0 \leq \chi_n \leq 1$ implies none of the corner points lie outside the region $\frac{\lambda_{\hat{n}}(1-p_{\hat{n}})}{p_{\hat{n}}} \geq \frac{\lambda_n(1-p_n)}{p_n} \geq 0$. Hence, for all $n \in \mathcal{M} \setminus \{\hat{n}\}$, $\frac{\lambda_{\hat{n}}(1-p_{\hat{n}})}{p_{\hat{n}}} = \frac{\lambda_n(1-p_n)}{p_n}$ and $\frac{\lambda_n(1-p_n)}{p_n} = 0$ are the boundaries of both $\overline{R}_{\hat{n}}$ and $\mathcal{H}_{\hat{n}}$. Therefore, from Lemma 2, $\overline{\mathcal{R}}_{\hat{n}} \subseteq \mathcal{H}_{\hat{n}}$, and $\overline{\mathcal{R}} = \bigcup_{\hat{n} \in \mathcal{M}} \overline{\mathcal{R}}_{\hat{n}} \subseteq \bigcup_{\hat{n} \in \mathcal{M}} \mathcal{H}_{\hat{n}} = \overline{\mathcal{H}}$. Since the boundaries $\frac{\lambda_{\hat{n}}(1-p_{\hat{n}})}{p_{\hat{n}}} = \frac{\lambda_n(1-p_n)}{p_n}$ and $\frac{\lambda_n(1-p_n)}{p_n} = 0$ are linear and the convex hull generated by a set of points is piecewise linear, $\overline{\mathcal{H}}$ is piecewise linear. ■

APPENDIX E
PROOF OF THEOREM 3

Notice that $\mathcal{H}$ is the convex hull of $\overline{\mathcal{H}}$. Since the union of convex sets need not be convex, it is trivial to see that $\overline{\mathcal{H}} \subseteq \mathcal{H}$. Therefore from Theorem 2, $\overline{\mathcal{R}} \subseteq \mathcal{H}$. By the same reason as in proving Theorem 2, $\mathcal{H}$ is also piecewise linear. ■

APPENDIX F
PROOF OF THEOREM 4

Introduce the following notations:

$$p^{\mathcal{M}}_{(x,y)} = \prod_{n' \in \mathcal{M} \setminus \{x,y\}} \overline{p}_{n'},$$
$$p^{\mathcal{M}}_{(x)} = \prod_{n' \in \mathcal{M} \setminus \{x\}} \overline{p}_{n'}.$$

Then, for each $\bar{n} \in \mathcal{M}$, $\Pi^{\mathsf{p}^{\mathcal{M}}(\mathcal{M}\setminus\{\bar{n}\})} = \left(\Pi^{\mathsf{p}^{\mathcal{M}}(\mathcal{M}\setminus\{\bar{n}\})}_n\right)_{n \in \mathcal{M}}$ is a point in M-dimensional space with

$$\Pi^{\mathsf{p}^{\mathcal{M}}(\mathcal{M}\setminus\{\bar{n}\})}_n = \begin{cases} p_n p^{\mathcal{M}}_{(n,\bar{n})}, & n \neq \bar{n} \\ 0, & n = \bar{n} \end{cases},$$

and $\Pi^{\mathsf{p}^{\mathcal{M}}(\mathcal{M})} = \left(\Pi^{\mathsf{p}^{\mathcal{M}}(\mathcal{M})}_n\right)_{n \in \mathcal{M}}$ is another point with

$$\Pi^{\mathsf{p}^{\mathcal{M}}(\mathcal{M})}_n = p_n p^{\mathcal{M}}_{(n)}, \forall n \in \mathcal{M}.$$

To determine whether the stability region of FRASA is $\boldsymbol{p}$-convex, we need the following two Lemmas.

Lemma 3: Let $\mathcal{X}_{\mathcal{M}}$ be a $M \times M$ matrix, with the first row equals $\mathbf{0} - \Pi^{\mathsf{p}^{\mathcal{M}}(\mathcal{M}\setminus\{1\})}$, and for $n \in \mathcal{M} \setminus \{1\}$, the n-th row is $\Pi^{\mathsf{p}^{\mathcal{M}}(\mathcal{M}\setminus\{n\})} - \Pi^{\mathsf{p}^{\mathcal{M}}(\mathcal{M}\setminus\{1\})}$. Then

$$\left|\mathcal{X}_{\mathcal{M}}\right| = (-1)^M (M-1) \prod_{n' \in \mathcal{M}} p_{n'} \prod_{n'' \in \mathcal{M}} \overline{p}^{M-2}_{n''}. \quad (15)$$

Lemma 4: Let $\mathcal{Y}_{\mathcal{M}}$ be a $M \times M$ matrix, with the first row equals $\Pi^{\mathsf{p}^{\mathcal{M}}(\mathcal{M})} - \Pi^{\mathsf{p}^{\mathcal{M}}(\mathcal{M}\setminus\{1\})}$, and for $n \in \mathcal{M} \setminus \{1\}$, the n-th row is $\Pi^{\mathsf{p}^{\mathcal{M}}(\mathcal{M}\setminus\{n\})} - \Pi^{\mathsf{p}^{\mathcal{M}}(\mathcal{M}\setminus\{1\})}$. Then

$$\left|\mathcal{Y}_{\mathcal{M}}\right| = (-1)^M \left(\sum_{n \in \mathcal{M}} p_n - 1\right) \prod_{n' \in \mathcal{M}} p_{n'} \prod_{n'' \in \mathcal{M}} \overline{p}^{M-2}_{n''}. \quad (16)$$

$\left|\mathcal{X}_{\mathcal{M}}\right|$ is calculated as follows:

$$\begin{aligned} \left|\mathcal{X}_{\mathcal{M}}\right| &= -\begin{vmatrix} 0 & p_2 p^{\mathcal{M}}_{(2,1)} & \cdots & p_M p^{\mathcal{M}}_{(M,1)} \\ p_1 p^{\mathcal{M}}_{(1,2)} & 0 & \cdots & p_M p^{\mathcal{M}}_{(M,2)} \\ \vdots & \vdots & \ddots & \vdots \\ p_1 p^{\mathcal{M}}_{(1,M)} & p_2 p^{\mathcal{M}}_{(2,M)} & \cdots & 0 \end{vmatrix} \\ &= -\prod_{n' \in \mathcal{M}} p_{n'} \prod_{n'' \in \mathcal{M}} \overline{p}^{M-2}_{n''} \begin{vmatrix} 0 & 1 & \cdots & 1 \\ 1 & 0 & \cdots & 1 \\ \vdots & \vdots & \ddots & \vdots \\ 1 & 1 & \cdots & 0 \end{vmatrix} \\ &= (-1)^M (M-1) \prod_{n' \in \mathcal{M}} p_{n'} \prod_{n'' \in \mathcal{M}} \overline{p}^{M-2}_{n''} \end{aligned}$$

The first equality is obtained by subtracting the first row of $\mathcal{X}_{\mathcal{M}}$ from all other rows in $\mathcal{X}_{\mathcal{M}}$. The second equality results from the observation that if for all $n'' \in \mathcal{M}$ we multiply $\overline{p}_{n''}$ to both the n''-th row and column, then we have a factor of $\prod_{n'' \in \mathcal{M}} \overline{p}_{n''}$ from each element in $\mathcal{X}_{\mathcal{M}}$. $\left|\mathcal{Y}_{\mathcal{M}}\right|$ is obtained similarly as shown below:

$$\begin{aligned} \left|\mathcal{Y}_{\mathcal{M}}\right| &= -\begin{vmatrix} -p_1 p^{\mathcal{M}}_{(1)} & p_1 p_2 p^{\mathcal{M}}_{(2,1)} & \cdots & p_1 p_M p^{\mathcal{M}}_{(M,1)} \\ p_2 p_1 p^{\mathcal{M}}_{(1,2)} & -p_2 p^{\mathcal{M}}_{(2)} & \cdots & p_2 p_M p^{\mathcal{M}}_{(M,2)} \\ \vdots & \vdots & \ddots & \vdots \\ p_M p_1 p^{\mathcal{M}}_{(1,M)} & p_M p_2 p^{\mathcal{M}}_{(2,M)} & \cdots & -p_M p^{\mathcal{M}}_{(M)} \end{vmatrix} \\ &= -\prod_{n' \in \mathcal{M}} p_{n'} \prod_{n'' \in \mathcal{M}} \overline{p}^{M-2}_{n''} \begin{vmatrix} -\overline{p}_1 & p_1 & \cdots & p_1 \\ p_2 & -\overline{p}_2 & \cdots & p_2 \\ \vdots & \vdots & \ddots & \vdots \\ p_M & p_M & \cdots & -\overline{p}_M \end{vmatrix} \\ &= (-1)^M \left(\sum_{n \in \mathcal{M}} p_n - 1\right) \prod_{n' \in \mathcal{M}} p_{n'} \prod_{n'' \in \mathcal{M}} \overline{p}^{M-2}_{n''} \end{aligned}$$

The proof of Theorem 4 goes as follows. We first construct a normal vector perpendicular to the hyperplane $\Omega^{\mathcal{M}}$. If we let $\{\mathbf{e}_n\}_{n \in \mathcal{M}}$ be the set of basis vector where $\mathbf{e}_n$ is a unit vector in the direction of increasing λ_n, then

$$\mathbf{n} = \begin{vmatrix} \mathbf{e}_1 & \mathbf{e}_2 & \cdots & \mathbf{e}_n \\ \mathrm{N}^2_1 & \mathrm{N}^2_2 & \cdots & \mathrm{N}^2_M \\ \vdots & \vdots & \ddots & \vdots \\ \mathrm{N}^M_1 & \mathrm{N}^M_2 & \cdots & \mathrm{N}^M_M \end{vmatrix}$$

with

$$\mathrm{N}^{\bar{n}}_n = \Pi^{\mathsf{p}^{\mathcal{M}}(\mathcal{M}\setminus\{\bar{n}\})}_n - \Pi^{\mathsf{p}^{\mathcal{M}}(\mathcal{M}\setminus\{1\})}_n$$

will be a normal vector of $\Omega^{\mathcal{M}}$. Therefore, $\left|\mathcal{X}_{\mathcal{M}}\right|$ is the inner product of $\mathbf{0} - \Pi^{\mathsf{p}^{\mathcal{M}}(\mathcal{M}\setminus\{1\})}$ and $\mathbf{n}$, while $\left|\mathcal{Y}_{\mathcal{M}}\right|$ is the inner product of $\Pi^{\mathsf{p}^{\mathcal{M}}(\mathcal{M})} - \Pi^{\mathsf{p}^{\mathcal{M}}(\mathcal{M}\setminus\{1\})}$ and $\mathbf{n}$. $\Pi^{\mathsf{p}^{\mathcal{M}}(\mathcal{M})}$ lies on $\Omega^{\mathcal{M}}$ is equivalent to $\left|\mathcal{Y}_{\mathcal{M}}\right| = 0$. $\Pi^{\mathsf{p}^{\mathcal{M}}(\mathcal{M})}$ and $\mathbf{0}$ lie on opposite sides of $\Omega^{\mathcal{M}}$ is equivalent to that $\left|\mathcal{X}_{\mathcal{M}}\right|$ and $\left|\mathcal{Y}_{\mathcal{M}}\right|$ have

opposite signs. With the condition that $\mathbf{0}$ never lies on $\Omega^{\mathcal{M}}$, $\boldsymbol{p}$-convexity is achieved if and only if $\left|\mathcal{X}_{\mathcal{M}}\right|\left|\mathcal{Y}_{\mathcal{M}}\right| \leq 0$. From Lemmas 3 and 4, the condition is equivalent to

$$(-1)^{2M}(M-1)\left(\sum_{n\in\mathcal{M}} p_n - 1\right)\prod_{n'\in\mathcal{M}} p_{n'}^2 \prod_{n''\in\mathcal{M}} \overline{p}_{n''}^{2(M-2)} \leq 0.$$

After simplification, it reduces to (11). ■

APPENDIX G
PROOF OF THEOREM 5

Notice that $\mathcal{H}$ is the convex hull of $\overline{\mathcal{H}}$. The corner points either lie on the boundary of $\mathcal{H}$ or in the interior of $\mathcal{H}$. If the stability region of FRASA is $\boldsymbol{p}$-convex, we only need to show that all corner points lie on the boundary of $\mathcal{H}$. It is because if all corner points are on the boundary of $\mathcal{H}$, then the union $\bigcup_{\hat{n}\in\mathcal{M}} \mathcal{H}_{\hat{n}}$ is convex and hence $\overline{\mathcal{H}} = \mathcal{H}$. Consider $M = 2$. When forming the convex hull $\mathcal{H}$, either

1) $\Pi^{\mathsf{p}^{\mathcal{M}}(\mathcal{M})}$ lies on $\Omega^{\mathcal{M}}$, meaning that $\Omega^{\mathcal{M}}$ is part of the boundary of $\mathcal{H}$; or
2) $\Pi^{\mathsf{p}^{\mathcal{M}}(\mathcal{M})}$ and $\mathbf{0}$ lie on opposite sides of $\Omega^{\mathcal{M}}$, which means $\Omega^{\mathcal{M}}$ will not be the boundary of $\mathcal{H}$ because there is a corner point $\Pi^{\mathsf{p}^{\mathcal{M}}(\mathcal{M})}$ lying beyond $\Omega^{\mathcal{M}}$.

In both cases, $\Pi^{\mathsf{p}^{\mathcal{M}}(\mathcal{M})}$ lies on the boundary of $\mathcal{H}$. For general values of M greater than two, we consider all $\mathcal{M}' \subseteq \mathcal{M}$ where $2 \leq |\mathcal{M}'| < M$ in ascending order of $|\mathcal{M}'|$. Because the stability region of FRASA with link set $\mathcal{M}'$ is also $\boldsymbol{p}$-convex, by repeating the arguments as above, we see that now all corner points except $\Pi^{\mathsf{p}^{\mathcal{M}}(\mathcal{M})}$ are on the boundary of $\mathcal{H}$ and $\Omega^{\mathcal{M}}$ is the boundary of the stability region farthest away from $\mathbf{0}$. Now we consider the corner point $\Pi^{\mathsf{p}^{\mathcal{M}}(\mathcal{M})}$. We can apply similar arguments as above to show that $\Pi^{\mathsf{p}^{\mathcal{M}}(\mathcal{M})}$ lies on the boundary of $\mathcal{H}$. Hence, $\overline{\mathcal{H}} = \mathcal{H}$. On the other hand, if the stability region of FRASA is not $\boldsymbol{p}$-convex, then $\Pi^{\mathsf{p}^{\mathcal{M}}(\mathcal{M})}$ lies in between $\mathbf{0}$ and $\Omega^{\mathcal{M}}$. Therefore, at least one corner point does not lie on the boundary of $\mathcal{H}$ and $\overline{\mathcal{H}} \subsetneq \mathcal{H}$. ■

APPENDIX H
PROOF OF THEOREM 6

Consider the bound of convex hull union $\overline{\mathcal{H}}$ in Theorem 2. Choose an arbitrary $\hat{n} \in \mathcal{M}$. When $\overline{\mathcal{H}}$ is intersected with the closed half space $\mathcal{S}_{\hat{n}}$, the resultant polytope does not contain the convex hull $\mathsf{H}_{\hat{n}}$ by construction. Therefore, this resultant polytope excludes the hypersurface $\mathsf{F}_{\hat{n}}$. We repeat this argument for all $\hat{n} \in \mathcal{M}$, then for all $\hat{n} \in \mathcal{M}$, the convex hull $\mathsf{H}_{\hat{n}}$ together with the hypersurface $\mathsf{F}_{\hat{n}}$ are removed. The boundary of the resultant polytope is consisted of $\mathsf{P}_{\hat{n}}$ for all $\hat{n} \in \mathcal{M}$ and the boundary of the positive orthant only, and hence the polytope is $\mathcal{S}$. Therefore, $\mathcal{S}$ is a subset of $\overline{\mathcal{R}}$ and constitutes an inner bound on the stability region of FRASA. This bound is convex and piecewise linear since half spaces are convex and piecewise linear, and these two properties are preserved under intersection. ■

REFERENCES

[1] B. S. Tsybakov and V. A. Mikhailov, "Ergodicity of a Slotted ALOHA System," *Probl. Inform. Transm.*, vol. 15, no. 4, pp. 73–87, 1979.

[2] R. R. Rao and A. Ephremides, "On the Stability of Interacting Queues in a Multiple-Access System," *IEEE Trans. Inf. Theory*, vol. 34, no. 5, pp. 918–930, Sep. 1988.

[3] W. Szpankowski, "Stability Conditions for Multidimensional Queueing Systems with Computer Applications," *Oper. Res.*, vol. 36, no. 6, pp. 944–957, Nov./Dec. 1988.

[4] V. Anantharam, "The Stability Region of the Finite-User Slotted ALOHA Protocol," *IEEE Trans. Inf. Theory*, vol. 37, no. 3, pp. 535–540, May 1991.

[5] W. Szpankowski, "Stability Conditions for Some Multiqueue Distributed Systems: Buffered Random Access Systems," *Adv. Appl. Probab.*, vol. 26, pp. 498–515, Jun. 1994.

[6] W. Luo and A. Ephremides, "Stability of N Interacting Queues in Random-Access Systems," *IEEE Trans. Inf. Theory*, vol. 45, no. 5, pp. 1579–1587, Jul. 1999.

[7] S. Ghez, S. Verdú, and S. C. Schwartz, "Stability Properties of Slotted Aloha With Multipacket Reception Capability," *IEEE Trans. Autom. Control*, vol. 33, no. 7, pp. 640–649, Jul. 1988.

[8] V. Naware, G. Mergen, and L. Tong, "Stability and Delay of Finite-User Slotted ALOHA With Multipacket Reception," *IEEE Trans. Inf. Theory*, vol. 51, no. 7, pp. 2636–2656, Jul. 2005.

[9] J. Luo and A. Ephremides, "On the Throughput, Capacity and Stability Regions of Random Multiple Access," *IEEE Trans. Inf. Theory*, vol. 52, no. 6, pp. 2593–2607, Jun. 2006.

[10] C. Bordenave, D. McDonald, and A. Proutiere, "Performance of Random Medium Access Control An Asymptotic Approach," in *2008 ACM SIGMETRICS International Conference on Measurement and Modeling of Computer Systems*, Annapolis, MD, Jun. 2008, pp. 1–12.

[11] N. Xie and S. Weber, "Geometric Approximations of Some ALOHA-like Stability Regions," in *2010 IEEE International Symposium on Information Theory*, Austin, TX, Jun. 2010, pp. 1848–1852.

[12] K.-H. Hui, W.-C. Lau, and O.-C. Yue, "Stability of Finite-User Slotted ALOHA under Partial Interference in Wireless Mesh Networks," in *PIMRC 2007*, Athens, Greece, Sep. 2007.

[13] ——, "Partial Interference and Its Performance Impact on Wireless Multiple Access Networks," *EURASIP Journal on Wireless Communications and Networking*, vol. 2010, article ID 735083, 20 pages, 2010. doi:10.1155/2010/735083.

[14] R. K. Chang and S. Lam, "Per-Queue Stability Analysis of a Random Access System," *IEEE Trans. Autom. Control*, vol. 46, no. 9, pp. 1446–1470, Sep. 2001.

[15] S. S. Lam, "Store-and-Forward Buffer Requirements in a Packet Switching Network," *IEEE Trans. Commun.*, vol. 24, no. 4, Apr. 1976.

[16] R. M. Loynes, "The Stability of a Queue with Non-Independent Inter-arrival and Service Times," *Proc. Cambridge Phil. Soc.*, vol. 58, pp. 494–520, 1962.

[17] J. R. Wieland, R. Pasupathy, and B. W. Schmeiser, "Queueing-Network Stability: Simulation-Based Checking," in *Proceedings of the 2003 Winter Simulation Conference*, vol. 1, Dec. 2003, pp. 520–527.

[18] D. Kincaid and W. Cheney, *Numerical Analysis: Mathematics of Scientific Computing*, 3rd ed. Brooks/Cole, 2002.

[19] K.-H. Hui, O.-C. Yue, and W.-C. Lau, "FRASA: Feedback Retransmission Approximation for the Stability Region of Finite-User Slotted ALOHA," Tech. Rep., Oct. 2007.

[20] J.-S. Chang and C.-K. Yap, "A Polynomial Solution for Potato-Peeling and Other Polygon Inclusion and Enclosure Problems," in *25th Annual Symposium on Foundations of Computer Science*, Oct. 1984, pp. 408–416.